

Platelet C5aR1 Aggravates Myocardial Infarction through Platelet–Neutrophil Interactions and CXCL4-Dependent NET Release

Nicolas Schommer^{1,2,3,4,5*}, Shanshan Zhang^{2,3*}, Henry Nording^{9,10,11}, Manuela Sauter^{2,3,4,7}, Jacob von Eisebeck^{9,10,11}, Paul Schilf¹², Christian D. Sadik¹², Nancy Schanze^{2,3,4}, Nadine Gauchel⁸, Muataz Ali Hamad⁸, Krystin Krauel^{2,3,4}, Niklas Burkhard⁸, Lukas A. Heger⁸, Harald F. Langer^{2,3,4,6,7†}, Daniel Duerschmied^{2,3,4,7†}

¹Program in Cellular and Molecular Medicine, Boston Children's Hospital, Boston, MA 02115, USA.

²Department of Cardiology, Angiology, Haemostaseology and Medical Intensive Care, University Medical Centre Mannheim, Medical Faculty Mannheim, Heidelberg University, Germany

³European Center for AngioScience (ECAS), Medical Faculty Mannheim, University of Heidelberg, Mannheim, Germany

⁴Helmholtz-Institute for Translational AngioCardioScience (HI-TAC) of the Max Delbrück Center for Molecular Medicine in the Helmholtz Association (MDC) at Heidelberg University, Heidelberg 69117, Germany

⁵Department of Pediatrics, Harvard Medical School, Boston, MA 02115, USA.

⁶Cardiovascular Systems Biology, Medical Faculty Mannheim, University of Heidelberg, Mannheim, Germany

⁷German Center for Cardiovascular Research (DZHK), Partner site Heidelberg/ Mannheim, Germany

⁸Department of Cardiology and Angiology, Heart Center, University Hospital Freiburg, University of Freiburg

⁹Cardioimmunology Group, Medical Clinic II, University Heart Center Lübeck, 23538 Lübeck, Germany.

¹⁰DZHK (German Centre for Cardiovascular Research), partner site Hamburg/Lübeck/Kiel, 23562 Lübeck, Germany.

¹¹Department of Internal Medicine V, Angiology, University of Kiel

¹²Department of Dermatology, Allergy, and Venereology, University of Lübeck, Lübeck, Germany

*, †These authors contributed equally to this work.

†Corresponding Authors:

Prof. Dr. Daniel Duerschmied

Medical Centre Mannheim, Medical Faculty Mannheim, Heidelberg University, Germany

Daniel.duerschmied@umm.de

Prof. Dr. Harald F. Langer

Medical Centre Mannheim, Medical Faculty Mannheim, Heidelberg University, Germany

Harald.langer@umm.de

Nonstandard Abbreviations and Acronyms

ANCA	anti-neutrophil cytoplasmic antibody
C3a	complement component 3a
C3aR	C3a receptor
C5	complement component 5
C5a	complement component 5a
C5aR1	C5a receptor 1
CXCL4	C-X-C motif chemokine ligand 4 (platelet factor 4)
GP1Ib/IIIa	glycoprotein IIb/IIIa (integrin α IIb β 3)
GPVI	glycoprotein VI
H3Cit	citrullinated histone H3
IL-1 β	interleukin-1 beta
LAD	left anterior descending (coronary artery)
Ly6G	lymphocyte antigen 6 complex, locus G
MAC-1	macrophage-1 antigen (integrin CD11b/CD18)
MI	myocardial infarction
MPO	myeloperoxidase
NET	neutrophil extracellular trap
NETosis	process of NET formation
PBS	phosphate-buffered saline
Pf4	platelet factor 4
Pf4-Cre	platelet factor 4 promoter-driven Cre recombinase
PMA	phorbol 12-myristate 13-acetate
PMC	platelet–monocyte complex
PNC	platelet–neutrophil complex
PMX205	small-molecule <i>C5ar1</i> antagonist
PSGL-1	P-selectin glycoprotein ligand-1
STEMI	ST-elevation myocardial infarction
TTC	2,3,5-triphenyltetrazolium chloride

VWF von Willebrand factor

WT wild-type

Short Title (running title): Platelet C5aR1 in Myocardial Infarction

Abstract

Platelet activation is a central driver of myocardial infarction. The complement anaphylatoxin C5a is abundantly generated during myocardial infarction, and its receptor C5aR1 is highly expressed on platelets. However, the functional role of platelet C5aR1 in myocardial infarction remains unknown. Here, we show that platelet-expressed C5aR1 critically amplifies thromboinflammatory cardiac injury by promoting platelet-mediated neutrophil activation after MI. Platelet-specific C5aR1 deletion reduced infarct size, fibrosis, and adverse remodeling while enhancing neovascularization and preserving cardiac function. Mechanistically, cell-specific C5aR1 deletion markedly reduced myocardial platelet–neutrophil accumulation and neutrophil extracellular trap (NET) formation, while circulating platelet–neutrophil complexes were increased. Ex vivo, C5a-stimulated platelets robustly induced NET release from neutrophils in a platelet C5aR1– and CXCL4–dependent manner, whereas platelets lacking C5aR1 failed to trigger NET formation. Pharmacological C5aR1 inhibition with PMX205 phenocopied the genetic platelet-specific deletion, resulting in comparable cardioprotection. Together, these findings identify platelet C5aR1 as a druggable target of platelet–neutrophil–NET signaling that exacerbates myocardial injury and limits reparative healing after MI, highlighting platelet C5aR1 as a potential therapeutic approach to restrain thromboinflammation.

Introduction

Myocardial infarction (MI) remains the leading cause of morbidity and mortality worldwide. Beyond acute coronary occlusion and thrombus formation, maladaptive inflammation critically determines infarct size and healing (1). The complement system is an evolutionarily conserved arm of the innate immune system that safeguards tissue integrity. Activated via the classical, lectin, or alternative pathway, it mediates opsonization and immune complex clearance, culminates in the formation of the membrane attack complex (C5b–C9) and cleaves the anaphylatoxins C3a and C5a (2).

C5a is a potent chemoattractant and activator of myeloid cells, particularly of neutrophils (3). Recent work from our group has revealed its expression on platelets, where it regulates vascular inflammation and ischemic neovascularization (4,5). Notably, platelet expression of C5aR1 and C3aR are increased in patients with coronary artery disease and show a strong correlation with platelet activation markers such as P-selectin (6), underscoring the potential clinical relevance of platelet complement signaling. These findings position platelets not only as effectors of thrombosis and hemostasis but also as active participants in innate immune responses involving complement signaling and tissue repair.

Beyond their hemostatic function, platelets patrol the vasculature as immune sentinels and dynamically engage with leukocytes (7–10). Among these, neutrophils represent a particularly relevant cellular partner in ischemic injury (11). Upon vascular damage or ischemia-reperfusion, platelets can rapidly form heterotypic complexes with neutrophils (platelet-neutrophil complexes, PNCs) and shape neutrophil activation through direct adhesive ligands and the release of soluble mediators (12,13).

Importantly, platelet signals can trigger neutrophil extracellular trap (NET) release, linking thrombosis with inflammation, vascular damage and fibrosis (14–16). NETs are web-like chromatin structures decorated with histones and proteases contributing to host defense (17). In sterile injury, however, they aggravate tissue damage by providing scaffolds for thrombosis, releasing cytotoxic mediators, and exposing neoantigens that may fuel autoimmunity (18,19). In myocardial infarction, intracardiac NET burden correlates with adverse remodeling, and experimental blockade of NETosis limits infarct size, inflammation, and fibrosis (20,21). Previous work has shown that excessive NET formation also promotes maladaptive cardiac remodeling in obesity (22), autoimmune disease (23), advanced age (24), and diabetes (25), underscoring their broad relevance as central drivers of thromboinflammation

and cardiovascular injury (18). The detection of NETs in failing human myocardium further highlights their relevance across acute and chronic heart disease (25–27). These insights suggest that complement, platelet–neutrophil complexes, and NETs could act as converging drivers of ischemic pathology. However, whether platelet-derived complement signaling through C5aR1, controls PNC formation and neutrophil effector functions in myocardial infarction remains unknown. Here, we investigated whether platelet-expressed C5aR1 orchestrates platelet–neutrophil interactions and NET formation to exacerbate myocardial injury and impair infarct healing.

Results

Platelet-specific *C5ar1* deletion improves post-infarction remodeling and cardiac function

Although systemic inhibition of C5 or C5aR1 has shown limited benefit in clinical trials of myocardial infarction, this may in part reflect the pleiotropic roles of complement across multiple different cell types (28–30). Global blockade can dampen both detrimental and reparative pathways, potentially masking cell-specific contributions. Our recent work demonstrated that platelet-expressed *C5ar1* regulates vascular inflammation and neovascularization in hindlimb ischemia through CXCL4 (4).

To define the role of platelet expressed *C5ar1* after myocardial infarction, Pf4^{cre+} *C5ar1*^{fl/fl} mice (4) and littermate controls underwent permanent LAD ligation (day 0), followed by serial echocardiographic assessment on days 1 and 13, flow cytometric analyses on days 1 and 14, and terminal analyses on day 14 (Figure 1A). TTC staining demonstrated 36% smaller infarct sizes in platelet-specific *C5ar1* knockouts compared to littermates (Figure 1B, C). Echocardiography confirmed improved systolic function in platelet *C5ar1*-deficient mice, with a 27% higher ejection fraction and 2-fold increased fractional shortening on day 13 (Figure 1D, E). Histological analyses revealed diminished collagen I deposition and reduced interstitial fibrosis in Pf4^{cre+} *C5ar1*^{fl/fl} hearts (Figure 1F, G). In addition to reduced fibrosis, Pf4^{cre+} *C5ar1*^{fl/fl} hearts exhibited a 5-fold increased capillary density in the peri-infarct zone, assessed by CD31 immunostaining (Figure 1H, I). These data indicate that platelet *C5ar1* deficiency not only limits injury and fibrosis but also favors adaptive neovascular remodeling after myocardial infarction, consistent with our prior observations in hindlimb ischemia (4). Together, these findings demonstrate that platelet-specific *C5ar1* deletion limits myocardial injury, improves functional recovery, and attenuates post-infarction remodeling.

Platelet *C5ar1* deficiency limits myocardial platelet–neutrophil complexes and NET deposition while increasing PNCs in blood

Given the pivotal role of platelet–neutrophil interactions in myocardial injury (12), we next investigated how platelet *C5ar1* influences PNC formation. Immunofluorescence staining of left ventricular sections for Ly6G and CD42b revealed significantly reduced deposition of PNCs in Pf4^{Cre+} *C5ar1*^{fl/fl} hearts compared to littermate controls, accompanied by fewer infiltrating neutrophils and platelets overall (Figure 2A, B & Supplemental Figure 10D). Because platelet–neutrophil interactions are a critical trigger of neutrophil activation and the release of NETs (11,12), we next examined whether reduced

myocardial PNC accumulation translated into reduced NET deposition within the infarcted heart. Immunofluorescence staining for MPO and H3Cit revealed a marked reduction in NET formation in *Pf4^{Cre+} C5ar1^{fl/fl}* hearts after infarction (Figure 2C). Quantitative analysis confirmed significantly fewer H3Cit⁺ neutrophils and reduced NET burden in the peri-infarct zone compared with littermate controls (Figure 2D). Together, these findings indicate that platelet *C5ar1* is required for myocardial accumulation of platelet–neutrophil complexes and subsequent formation of NETs in the infarcted heart.

We next set out to investigate PNCs in the circulation as well. Unstimulated whole blood was analyzed by flow cytometry on days 1 and 14 after infarction (Figure 2E). As expected, PNCs rose sharply on day 1 and declined toward baseline by day 14 (Figure 2F). Unexpectedly, platelet-specific *C5ar1^{-/-}* mice had markedly higher circulating PNC levels on day 1 compared with littermate controls, despite their improved cardiac function and reduced PNC accumulation in tissue. Similar analyses of platelet–monocyte complexes (PMCs), quantified in blood by CD115/CD42b co-staining and in myocardium by CD68 immunofluorescence, revealed comparable temporal dynamics after infarction but no genotype-dependent differences (Supplemental Figure 2 & 14). To explore a potential relationship between early circulating platelet–neutrophil interactions and later myocardial PNC accumulation, we performed a correlation analysis. Notably, the proportion of circulating PNCs on day 1 inversely correlated with myocardial PNC burden on day 14 (Spearman $r = -0.83$; $P = 0.02$; Figure 2G), consistent with the notion that platelet *C5ar1* deficiency alters the spatial distribution of platelet–neutrophil interactions following myocardial infarction.

These findings suggest that in the absence of platelet *C5ar1*, PNCs form readily in the circulation but fail to accumulate and make NETs within injured myocardium. This effect appears specific to platelet–neutrophil interactions rather than platelet–leukocyte crosstalk in general.

Platelet *C5ar1* regulates α -granule biology and promotes CXCL4 dependent NET formation

To delineate the platelet-intrinsic mechanism linking *C5a/C5ar1* signaling to platelet neutrophil interactions and NET formation, we first examined whether *C5ar1* influences platelet α -granule biology at baseline. Immunofluorescence analysis of resting platelets revealed markedly reduced intracellular P-selectin (CD62P) signal in *C5ar1*-deficient platelets, when compared with WT platelets, indicating altered α -granule content or organization (Figure 3A, B). Because surface translocation of

P-selectin is a hallmark of platelet activation, a key mediator of PNC formation via PSGL-1 (12), and a well-established trigger of NETosis (14), we next assessed platelet activation after myocardial infarction via flow cytometry. Whole blood obtained 24 h after infarction was stimulated *ex vivo* with 100 nM phorbol 12-myristate 13-acetate (PMA). Under these conditions, platelets from Pf4^{Cre+} *C5ar1*^{fl/fl} mice exhibited reduced surface P-selectin expression (Figure 3C) and diminished activation of integrin GPIIb/IIIa (Figure 3D) compared with littermate controls, demonstrating impaired platelet activation downstream of platelet *C5ar1* signaling after MI.

Besides P-selectin, α -granule secretion also represents a major source of platelet-derived CXCL4 (platelet factor 4). Consistent with defective granule mobilization, plasma CXCL4 levels were significantly reduced in Pf4^{Cre+} *C5ar1*^{fl/fl} mice after MI (Figure 3E), indicating impaired platelet *C5ar1*-dependent CXCL4 release *in vivo*. We previously identified a platelet *C5a/C5ar1/CXCL4* axis in ischemia-driven neovascularization (4), which, together with recent reports implicating platelet-derived CXCL4 in NET formation in ANCA-associated vasculitis (31), prompted us to test whether CXCL4 could mediate platelet *C5ar1*-dependent NET formation downstream of *C5a*.

Neutrophils were co-incubated with WT or *C5ar1*-deficient platelets stimulated with *C5a* (Figure 3F), and NET formation was quantified by immunofluorescence staining for citrullinated histone H3 (H3Cit), myeloperoxidase (MPO), and DNA (DAPI). *C5a*-stimulated WT platelets robustly induced NET formation, whereas *C5a*-stimulated *C5ar1*-KO platelets failed to promote NET release (Figure 3G, H).

To directly test the requirement for CXCL4 in this, secreted CXCL4 was functionally neutralized using heparin, which binds platelet factor 4 with high affinity and sequesters it into inactive complexes (32,33). As hypothesized, heparin markedly attenuated NET formation induced by *C5a*-stimulated WT platelets (Figure 3G, H), demonstrating that active CXCL4 is required for platelet-driven NETosis downstream of *C5ar1*. We next asked whether restoring CXCL4 could rescue NET formation in the absence of platelet *C5ar1*. Adding recombinant CXCL4 (rCXCL4), indeed, fully restored NET formation in co-cultures containing *C5a*-stimulated KO platelets and neutrophils (Figure 3G, H), establishing CXCL4 as a sufficient mediator downstream of *C5a* resulting in NET formation.

Together, these findings place platelet *C5ar1* upstream of α -granule mobilization and CXCL4 release and identify CXCL4 as a critical mediator licensing platelet-dependent NET formation.

Pharmacological inhibition of C5aR1 phenocopies platelet-specific *C5ar1* deletion

To translate our findings into a therapeutic context, we next evaluated the small-molecule C5aR1 inhibitor PMX205 in the permanent LAD ligation model. Mice received daily subcutaneous injections of PMX205 or its vehicle PBS for 14 days after MI (Figure 4A). PMX205 treatment closely recapitulated the protective phenotype observed in platelet-specific *C5ar1*^{-/-} mice. TTC staining revealed a marked reduction in infarct size in PMX205-treated mice compared with controls (Figure 4B). Collagen I immunofluorescence confirmed decreased interstitial fibrosis in the infarct border zone (Figure 4C). Consistent with these structural improvements, echocardiography demonstrated enhanced systolic function, with higher ejection fraction and fractional shortening in PMX205-treated animals (Figure 4D, E). In line with the genetic deletion, PMX205 reduced platelet–neutrophil complexes and neutrophil accumulation in the infarcted myocardium (Figure 4F, G, Supplementary Figure 16B). Given the potent neutrophil chemoattractant properties of C5a (34,35), this decrease in neutrophil recruitment is consistent with effective systemic C5aR1 blockade. Platelet infiltration was likewise diminished in PMX205-treated hearts (Supplementary Figure 10). Moreover, tissue analyses demonstrated reduced myocardial NET burden in PMX205-treated mice (Figure 4H, I). Flow cytometric analyses revealed attenuated platelet activation, reflected by lower surface P-selectin expression and reduced GPIIb/IIIa activation (Figure 4J–L).

Together, these data demonstrate that pharmacological C5aR1 inhibition with PMX205 phenocopies platelet-specific *C5ar1* deletion, conferring robust cardioprotection and suppressing thromboinflammatory signaling after myocardial infarction. These findings highlight C5aR1 as a promising therapeutic target to limit platelet-driven inflammation and myocardial injury.

Discussion

This study identifies platelet-expressed C5aR1 as a central regulator of thromboinflammatory injury and myocardial repair following infarction. Using complementary genetic and pharmacological approaches, we demonstrate that platelet C5aR1 amplifies platelet–neutrophil interactions, platelet activation, and neutrophil extracellular trap (NET) formation via CXCL4 release, thereby increasing infarct size, fibrosis, and adverse ventricular remodeling. These findings establish platelet-intrinsic complement signaling as an upstream determinant of infarct healing and highlight platelet C5aR1 as a promising therapeutic hub.

Complement–platelet interactions have emerged as potent amplifiers of vascular inflammation in recent years (2,36). Beyond their hemostatic role, platelets actively regulate complement activation and sensing at sites of vascular injury, thereby coupling tissue damage to thromboinflammatory responses (2,4,5). Seminal work has demonstrated that platelet activation can initiate and propagate complement activation, positioning platelets as both targets and amplifiers of complement signaling (37–41).

Among complement receptors, the anaphylatoxin receptor C5aR1 is of particular interest, given its strong myeloid-activating capacity. C5a/C5aR1 signaling on leukocytes, especially on neutrophils, promotes recruitment, activation, and NET formation and aggravates myocardial injury, processes thus far considered largely platelet-independent (3,34,42). Our data uncover a novel platelet-centric pathway, showing that platelets themselves are a decisive C5aR1-expressing population that licenses pathogenic neutrophil effector functions after MI. The observed effects appear specific to platelet–neutrophil crosstalk, as platelet–monocyte complexes and monocyte infiltration remained unaffected.

This platelet–neutrophil–focused perspective is particularly relevant given the mixed translational experience with systemic complement inhibition in myocardial infarction. While blockade of C5 or C5aR1 confers robust cardioprotection in experimental models (34,42), clinical translation of systemic complement inhibition has yielded inconsistent benefit (28,29). These outcomes likely reflect the pleiotropic roles of C5a/C5aR1 across multiple cell types, where indiscriminate inhibition may suppress both deleterious and reparative immune functions required for infarct healing (43,44).

Thus, indiscriminate C5aR1 blockade may inadvertently impair beneficial neutrophil effector functions while curbing pathological activation. The observation that platelet C5aR1 (and C3aR) expression is increased in patients with coronary artery disease and acute ST-elevation myocardial infarction (6)

further underscores platelets as a clinically relevant C5aR1 compartment and supports the concept that cell-specific targeting may overcome the limitations of systemic complement inhibition.

Prior work identified platelet C5aR1 as a regulator of ischemic angiogenesis in peripheral artery disease via a C5a/CXCL4 axis (4). We now extend these insights to the infarcted heart, showing that platelet C5aR1 orchestrates both aggregate- and secretome-dependent pathways of platelet–neutrophil interaction that ultimately determine myocardial injury and repair.

A striking feature of our data is the divergence between circulating and tissue platelet–neutrophil complexes (PNCs). Platelet-specific C5aR1 deficiency increased circulating PNCs while markedly reducing their accumulation within the infarcted myocardium, accompanied by decreased platelet and neutrophil infiltration and reduced NET deposition overall. These findings indicate that C5aR1 is dispensable for complex formation per se but is required for their recruitment to ischemic tissue and subsequent pathogenic activation.

Mechanistically, loss of C5aR1 altered α -granule biology and blunted platelet activation early after myocardial infarction, as evidenced by reduced granule and surface P-selectin expression and diminished integrin GPIIb/IIIa activation. Consequently, PNCs fail to efficiently accumulate within ischemic myocardium. Multiple, partially overlapping platelet-derived pathways have been shown to promote NET formation, including adhesive interactions, granule-derived mediators, and innate immune sensing mechanisms (14,16,45). In this context, our data implicate CXCL4 as a downstream mediator of platelet C5a/C5aR1 signaling resulting in NETosis. While P-selectin provides a permissive adhesive scaffold for platelet–neutrophil complexes via PSGL-1 and is a well-known inducer of NETosis (12,14), platelet-specific C5aR1 deficiency reduced circulating CXCL4 levels, and platelet-mediated NET induction required intact C5a/C5aR1 signaling in a CXCL4-dependent manner in vitro. Recent evidence also points to platelet GPVI as an alternative pathway promoting platelet–neutrophil aggregates in acute lung injury (46); such mechanisms may partially compensate for the loss of integrin-dependent signaling in *C5ar1*-deficient platelets and help explain the persistence of circulating PNCs. Consistent with our findings, platelet-derived CXCL4 has previously been shown to promote NETosis in autoimmune diseases such as ANCA-associated vasculitis (31), suggesting broader relevance for this pathway.

Thus, platelet C5aR1 acts as a molecular switch that governs not the abundance but the pathogenic quality and fate of platelet–neutrophil aggregates. These results resonate with earlier clinical

observations that platelet–leukocyte aggregates are elevated in acute coronary syndromes and predict adverse outcome (12,47,48).

Downstream, platelet C5aR1 proved essential for platelet-mediated NET induction. In the infarcted myocardium, NET burden was significantly lower in knockout mice, and platelets frequently colocalized with NETting neutrophils, underscoring their spatial proximity in this process.

NETs themselves are central drivers of infarct pathology: they aggravate ischemia/reperfusion injury (21,49), impair tissue healing (50), promote fibrosis (24), and drive maladaptive remodeling in myocardial infarction through neutrophil inflammasome–driven IL-1 β release and VWF deposition (20). By positioning platelet C5aR1 upstream of this pathway, our study identifies complement–platelet signaling as a critical initiator of the NET–fibrosis–remodeling cascade.

In addition to regulating platelet–neutrophil crosstalk, platelet C5aR1 shaped the paracrine environment of ischemic myocardium. CXCL4, beyond promoting NET formation (31), has been shown to suppress adaptive neovascularization in hindlimb ischemia (4). Consistent with this dual role, reduced CXCL4 levels in platelet-specific *C5ar1*^{-/-} mice coincided with increased capillary density in peri-infarct myocardium. These observations suggest that platelet C5aR1 simultaneously fuels thromboinflammatory injury while constraining reparative angiogenesis.

The therapeutic implications of these findings are considerable. Pharmacological blockade of C5aR1 with the small-molecule antagonist PMX205 phenocopied platelet-specific genetic deletion, resulting in smaller infarcts, improved systolic function, reduced platelet activation, diminished myocardial PNC accumulation, attenuated NET burden, and reduced fibrosis. Importantly, platelet C5aR1 deficiency preserved platelet counts and gross hemostatic function (4), consistent with a predominantly inflammatory role of platelet C5aR1 (unlike platelet C3aR, which also affects hemostasis and comes with inadvertent bleeding risks (51)). Although PMX205 is not cell-type selective, its ability to phenocopy platelet-specific C5aR1 deletion supports the principle that selectively uncoupling inflammatory complement signaling from hemostasis may be therapeutically exploitable.

Complement-targeted therapies have demonstrated clinical efficacy and safety across inflammatory diseases, establishing translational feasibility for selective modulation of complement signaling (52–54). Our findings extend this principle to acute myocardial infarction. In contrast to systemic complement blockade, platelet-restricted C5aR1 targeting may avoid blunting reparative immune functions that are required for proper infarct healing or immune defense.

Several limitations warrant consideration. Our analyses focused on later stages after infarction to capture the structural consequences of early thromboinflammatory signaling rather than acute platelet–neutrophil kinetics. Future studies incorporating earlier time points, reperfusion models, and human validation will be required to fully resolve the temporal hierarchy and translational relevance of platelet C5aR1–dependent signaling.

Together, these findings identify platelet C5aR1 as a central molecular switch that determines whether platelet–neutrophil interactions remain benign or evolve into pathogenic drivers of NET formation, impaired angiogenesis, and fibrotic remodeling after myocardial infarction. By positioning platelet C5aR1 upstream of CXCL4–dependent neutrophil activation and thromboinflammatory injury, this study defines a platelet-intrinsic complement pathway that integrates innate immune danger cues into maladaptive cardiac remodeling and highlights platelet C5aR1 as a rational therapeutic target to improve infarct healing.

Methods

Detailed descriptions of materials, reagents, and extended experimental protocols are provided in the Supplementary Methods. Data supporting the findings of this study are available from the corresponding authors upon reasonable request.

Animal Models and Study Design

Platelet-specific *C5ar1*-deficient mice (*C5ar1^{fl/fl};Pf4-Cre⁺*) and Cre-negative littermate controls (*C5ar1^{fl/fl};Pf4-Cre⁻*) on a C57BL/6J background were used. Male mice aged 10–14 weeks were studied. All animal experiments were approved by the regional authorities of Baden-Württemberg (Regierungspräsidium Freiburg, approval no. 35-9185.81/G-20/105) and conducted in accordance with the German Animal Welfare Act.

Animals were followed for 24 h to assess acute thromboinflammatory responses and for 14 days to evaluate post-infarction remodeling. Echocardiography was performed on days 1 and 13, and hearts were harvested on day 14 for histological and molecular analyses. Investigators were blinded to genotype and treatment during data acquisition and analysis. The platelet-specific *C5ar1* knockout mouse line has been previously comprehensively characterized, including analyses of whole blood counts, platelet aggregation, bleeding time, and platelet activation (4).

Myocardial Infarction Model

Myocardial infarction was induced by permanent ligation of the left anterior descending (LAD) coronary artery under general anesthesia, endotracheal intubation, and mechanical ventilation. Successful coronary occlusion was confirmed by immediate blanching of the anterior left ventricular wall and characteristic wall motion abnormalities in echocardiography. Detailed surgical procedures, anesthesia, ventilation, and postoperative analgesia are described in the Supplementary Methods.

Pharmacological C5aR1 Blockade

For pharmacological inhibition experiments, wild-type mice only received the selective C5aR1 antagonist PMX205 (Tocris) or PBS vehicle. PMX205 was administered subcutaneously at 1 mg/kg body weight, first 4 h prior to LAD ligation and subsequently once daily until tissue harvest. The maximal injection volume was 10 μ L/g body weight.

Echocardiography

Transthoracic echocardiography was performed using a Vevo 3100 imaging system (FUJIFILM VisualSonics) with Vevo LAB software, equipped with a high-frequency linear array transducer (22–55 MHz) suitable for murine cardiac imaging. Examinations were conducted on day 1 and day 13 after myocardial infarction under light isoflurane anesthesia.

B-mode images were acquired from parasternal long-axis (PSLAX) and parasternal short-axis (SAX) views, followed by M-mode recordings obtained from both views at the mid-papillary level. Left ventricular dimensions were measured from M-mode images, and ejection fraction and fractional shortening were calculated as the primary functional parameters. Measurements were averaged from three consecutive cardiac cycles and analyzed by investigators blinded to genotype and treatment group.

Infarct Size and Cardiac Remodeling

Infarct size was determined by 2,3,5-triphenyltetrazolium chloride (TTC) staining. Hearts were sectioned into three 2-mm transverse slices distal to the ligation site, and infarct size was quantified as the ratio of non-viable to total myocardial area using ImageJ/Fiji. At 14 days, myocardial remodeling was assessed by immunofluorescence analysis of fibrosis (Collagen I) and neovascularization in infarct border zones.

Flow Cytometric Analysis of Platelet–Leukocyte Complexes and Platelet Activation

Platelet–neutrophil complexes (PNCs) and platelet–monocyte complexes (PMCs) were quantified in whole blood by flow cytometry on day 1 and day 14 after myocardial infarction. Platelets were identified as CD42b⁺ events and neutrophils as Ly6G⁺ cells. Platelet activation was assessed by surface expression of P-selectin and activated GPIIb/IIIa under basal conditions and following ex vivo stimulation with phorbol 12-myristate 13-acetate (PMA). Antibody panels, gating strategies, and stimulation conditions are detailed in the Supplementary Methods.

Detection of PNCs and NETs in Myocardial Tissue

Platelet–neutrophil complexes in myocardial tissue were visualized by immunofluorescence staining for platelet (CD42b) and neutrophil (Ly6G) markers. Neutrophil extracellular traps (NETs) were

identified by co-localization of extracellular DNA with citrullinated histone H3 (H3Cit) and myeloperoxidase (MPO). Quantification was performed in infarct and peri-infarct regions as described in the Supplementary Methods.

Platelet–Neutrophil Co-culture and NET Formation Assays

Bone marrow–derived neutrophils were co-incubated with isolated platelets. Co-cultures were stimulated with defined agonists, and NET formation was assessed by immunofluorescence detection of extracellular MPO⁺ H3cit⁺ DNA⁺ structures. NETs were quantified as the percentage of neutrophils positive for H3Cit and MPO. Detailed isolation procedures, stimulation conditions, permeabilization, staining protocols, and image analysis are provided in the Supplementary Methods.

CXCL4 Quantification

CXCL4 concentrations were measured in plasma samples using a mouse CXCL4 (platelet factor 4) Quantikine ELISA kit (R&D Systems, MCX400) according to the manufacturer's instructions.

Statistical Analysis

All data are expressed as mean \pm SD. Data distribution and homogeneity of variance were evaluated prior to selecting appropriate statistical tests. Comparisons between two independent samples were performed using unpaired t-tests, applying Welch's correction when variances differed, or Mann–Whitney U tests for non-parametric data. Analyses involving three or more groups employed one- or two-way ANOVA (with Welch's adjustment when required) followed by Tukey or Šidák post hoc tests, or Kruskal–Wallis testing with Dunn's post hoc correction. All tests were two-tailed, and significance was defined as $\alpha = 0.05$. Exact sample sizes, statistical tests, and p-values are detailed in the figure legends and Supplementary Tables.

References

1. Prabhu SD, Frangogiannis NG. The Biological Basis for Cardiac Repair After Myocardial Infarction: From Inflammation to Fibrosis. *Circ Res*. 2016;119(1):91–112.
2. Rawish E, Sauter M, Sauter R, Nording H, Langer HF. Complement, inflammation and thrombosis. *Br J Pharmacol*. 2021 July;178(14):2892–904.
3. Chen Y, Li X, Lin X, Liang H, Liu X, Zhang X, et al. Complement C5a induces the generation of neutrophil extracellular traps by inhibiting mitochondrial STAT3 to promote the development of arterial thrombosis. *Thromb J*. 2022 Dec;20(1):24.
4. Nording H, Baron L, Haberthür D, Emschermann F, Mezger M, Sauter M, et al. The C5a/C5a receptor 1 axis controls tissue neovascularization through CXCL4 release from platelets. *Nat Commun*. 2021 Dec;12(1):3352.
5. Nording H, Baron L, Sauter M, Lübken A, Rawish E, Szepanowski R, et al. Platelets regulate ischemia-induced revascularization and angiogenesis by secretion of growth factor–modulating factors. *Blood Adv*. 2023 Nov 14;7(21):6411–27.
6. Patzelt J, Mueller KAL, Breuning S, Karathanos A, Schleicher R, Seizer P, et al. Expression of anaphylatoxin receptors on platelets in patients with coronary heart disease. *Atherosclerosis*. 2015 Feb;238(2):289–95.
7. Von Hundelshausen P, Weber C. Platelets as Immune Cells: Bridging Inflammation and Cardiovascular Disease. *Circ Res*. 2007 Jan 5;100(1):27–40.
8. Langer HF. Platelets and Immune Responses During Thromboinflammation. *Front Immunol*. 2019;10:14.
9. Duerschmied D, Suidan GL, Demers M, Herr N, Carbo C, Brill A, et al. Platelet serotonin promotes the recruitment of neutrophils to sites of acute inflammation in mice. *Blood*. 2013 Feb 7;121(6):1008–15.
10. Mauler M, Herr N, Schoenichen C, Witsch T, Marchini T, Härdtner C, et al. Platelet Serotonin Aggravates Myocardial Ischemia/Reperfusion Injury via Neutrophil Degranulation. *Circulation*. 2019 Feb 12;139(7):918–31.
11. Denorme F, Rustad JL, Campbell RA. Brothers in arms: platelets and neutrophils in ischemic stroke. *Curr Opin Hematol*. 2021 Sept;28(5):301–7.

12. Han J, Bloxham CJ, Kirmes K, Viggiani G, Unkelbach LP, Von Scheidt M, et al. Platelet–leukocyte aggregates in cardiovascular disease: prognostic significance and therapeutic potential. *Cardiovasc Res*. 2025 Sept 29;121(11):1679–96.
13. Mauler M, Seyfert J, Haenel D, Seeba H, Guenther J, Stallmann D, et al. Platelet-neutrophil complex formation—a detailed in vitro analysis of murine and human blood samples. *J Leukoc Biol*. 2016 May 1;99(5):781–9.
14. Etulain J, Martinod K, Wong SL, Cifuni SM, Schattner M, Wagner DD. P-selectin promotes neutrophil extracellular trap formation in mice. *Blood*. 2015 July 9;126(2):242–6.
15. Clark SR, Ma AC, Tavener SA, McDonald B, Goodarzi Z, Kelly MM, et al. Platelet TLR4 activates neutrophil extracellular traps to ensnare bacteria in septic blood. *Nat Med*. 2007 Apr;13(4):463–9.
16. Denorme F, Portier I, Rustad JL, Cody MJ, De Araujo CV, Hoki C, et al. Neutrophil extracellular traps regulate ischemic stroke brain injury. *J Clin Invest*. 2022 May 16;132(10):e154225.
17. Brinkmann V, Reichard U, Goosmann C, Fauler B, Uhlemann Y, Weiss DS, et al. Neutrophil Extracellular Traps Kill Bacteria. *Science*. 2004 Mar 5;303(5663):1532–5.
18. Wagner DD, Heger LA. Thromboinflammation: From Atherosclerosis to COVID-19. *Arterioscler Thromb Vasc Biol*. 2022 Sept;42(9):1103–12.
19. Wang Y, Xiao Y, Zhong L, Ye D, Zhang J, Tu Y, et al. Increased Neutrophil Elastase and Proteinase 3 and Augmented NETosis Are Closely Associated With β -Cell Autoimmunity in Patients With Type 1 Diabetes. *Diabetes*. 2014 Dec 1;63(12):4239–48.
20. Heger LA, Schommer N, Van Bruggen S, Sheehy CE, Chan W, Wagner DD. Neutrophil NLRP3 promotes cardiac injury following acute myocardial infarction through IL-1 β production, VWF release and NET deposition in the myocardium. *Sci Rep*. 2024 June 24;14(1):14524.
21. Savchenko AS, Borissoff JI, Martinod K, De Meyer SF, Gallant M, Erpenbeck L, et al. VWF-mediated leukocyte recruitment with chromatin decondensation by PAD4 increases myocardial ischemia/reperfusion injury in mice. *Blood*. 2014 Jan 2;123(1):141–8.
22. Van Bruggen S, Sheehy CE, Kraisin S, Frederix L, Wagner DD, Martinod K. Neutrophil peptidylarginine deiminase 4 plays a systemic role in obesity-induced chronic inflammation in mice. *J Thromb Haemost*. 2024 May;22(5):1496–509.

23. Heger LA, Schommer N, Fukui S, Van Bruggen S, Sheehy CE, Chu L, et al. Inhibition of protein arginine deiminase 4 prevents inflammation-mediated heart failure in arthritis. *Life Sci Alliance*. 2023 Oct;6(10):e202302055.
24. Martinod K, Witsch T, Erpenbeck L, Savchenko A, Hayashi H, Cherpokova D, et al. Peptidylarginine deiminase 4 promotes age-related organ fibrosis. *J Exp Med*. 2017 Feb 1;214(2):439–58.
25. Schommer N, Gendron N, Krauel K, Van Bruggen S, Jarrot PA, Maier A, et al. Neutrophil extracellular traps and peptidylarginine deiminase 4–mediated inflammasome activation link diabetes to cardiorenal injury and heart failure. *Eur Heart J*. 2025 Nov 27;ehaf963.
26. Ichimura S, Misaka T, Ogawara R, Tomita Y, Anzai F, Sato Y, et al. Neutrophil Extracellular Traps in Myocardial Tissue Drive Cardiac Dysfunction and Adverse Outcomes in Patients With Heart Failure With Dilated Cardiomyopathy. *Circ Heart Fail [Internet]*. 2024 June [cited 2024 Dec 16];17(6). Available from: <https://www.ahajournals.org/doi/10.1161/CIRCHEARTFAILURE.123.011057>
27. Kostin S, Richter M, Krizanic F, Sasko B, Kelesidis T, Pagonas N. NETosis is an Important Component of Chronic Myocardial Inflammation in Patients With Heart Failure. *Circ Heart Fail*. 2024 Nov 8;e012231.
28. Martel C, Granger CB, Ghitecu M, Stebbins A, Fortier A, Armstrong PW, et al. Pexelizumab fails to inhibit assembly of the terminal complement complex in patients with ST-elevation myocardial infarction undergoing primary percutaneous coronary intervention. Insight from a substudy of the Assessment of Pexelizumab in Acute Myocardial Infarction (APEX-AMI) trial. *Am Heart J*. 2012 July;164(1):43–51.
29. Pexelizumab for Acute ST-Elevation Myocardial Infarction in Patients Undergoing Primary Percutaneous Coronary Intervention: A Randomized Controlled Trial. *JAMA*. 2007 Jan 3;297(1):43.
30. Vakeva AP, Agah A, Rollins SA, Matis LA, Li L, Stahl GL. Myocardial Infarction and Apoptosis After Myocardial Ischemia and Reperfusion: Role of the Terminal Complement Components and Inhibition by Anti-C5 Therapy. *Circulation*. 1998 June 9;97(22):2259–67.
31. Matsumoto K, Yasuoka H, Yoshimoto K, Suzuki K, Takeuchi T. Platelet CXCL4 mediates neutrophil extracellular traps formation in ANCA-associated vasculitis. *Sci Rep*. 2021 Jan 8;11(1):222.

32. Mayo KH, Ilyina E, Roongta V, Dundas M, Joseph J, Lai CK, et al. Heparin binding to platelet factor-4. An NMR and site-directed mutagenesis study: arginine residues are crucial for binding. *Biochem J*. 1995 Dec 1;312(2):357–65.
33. Slungaard A, Key NS. Platelet factor 4 stimulates thrombomodulin protein C-activating cofactor activity. A structure-function analysis. *J Biol Chem*. 1994 Oct;269(41):25549–56.
34. Mueller M, Herzog C, Larmann J, Schmitz M, Hilfiker-Kleiner D, Gessner JE, et al. The receptor for activated complement factor 5 (C5aR) conveys myocardial ischemic damage by mediating neutrophil transmigration. *Immunobiology*. 2013 Sept;218(9):1131–8.
35. Gerard NP, Gerard C. The chemotactic receptor for human C5a anaphylatoxin. *Nature*. 1991 Feb;349(6310):614–7.
36. Nording H, Langer HF. Complement links platelets to innate immunity. *Semin Immunol*. 2018 June;37:43–52.
37. Del Conde I, Cruz MA, Zhang H, López JA, Afshar-Kharghan V. Platelet activation leads to activation and propagation of the complement system. *J Exp Med*. 2005 Mar 21;201(6):871–9.
38. Ekdahl KN, Nilsson B. Phosphorylation of complement component C3 and C3 fragments by a human platelet protein kinase. Inhibition of factor I-mediated cleavage of C3b. *J Immunol Baltim Md 1950*. 1995 June 15;154(12):6502–10.
39. Hamad OA, Nilsson PH, Wouters D, Lambris JD, Ekdahl KN, Nilsson B. Complement Component C3 Binds to Activated Normal Platelets without Preceding Proteolytic Activation and Promotes Binding to Complement Receptor 1. *J Immunol*. 2010 Mar 1;184(5):2686–92.
40. Subramaniam S, Jurk K, Hobohm L, Jäckel S, Saffarzadeh M, Schwierczek K, et al. Distinct contributions of complement factors to platelet activation and fibrin formation in venous thrombus development. *Blood*. 2017 Apr 20;129(16):2291–302.
41. Verschoor A, Neuenhahn M, Navarini AA, Graef P, Plaumann A, Seidlmeier A, et al. A platelet-mediated system for shuttling blood-borne bacteria to CD8 α ⁺ dendritic cells depends on glycoprotein GPIb and complement C3. *Nat Immunol*. 2011 Dec;12(12):1194–201.
42. De Hoog VC, Timmers L, Van Duijvenvoorde A, De Jager SCA, Van Middelaar BJ, Smeets MB, et al. Leucocyte expression of complement C5a receptors exacerbates infarct size after myocardial reperfusion injury. *Cardiovasc Res*. 2014 Sept 1;103(4):521–9.

43. Frangogiannis NG. The inflammatory response in myocardial injury, repair, and remodelling. *Nat Rev Cardiol.* 2014 May;11(5):255–65.
44. Ma Y. Role of Neutrophils in Cardiac Injury and Repair Following Myocardial Infarction. *Cells.* 2021 July 2;10(7):1676.
45. Clark SR, Ma AC, Tavener SA, McDonald B, Goodarzi Z, Kelly MM, et al. Platelet TLR4 activates neutrophil extracellular traps to ensnare bacteria in septic blood. *Nat Med.* 2007 Apr;13(4):463–9.
46. Burkard P, Schonhart C, Vögtle T, Köhler D, Tang L, Johnson D, et al. A key role for platelet GPVI in neutrophil recruitment, migration, and NETosis in the early stages of acute lung injury. *Blood.* 2023 Oct 26;142(17):1463–77.
47. Furman MI, Benoit SE, Barnard MR, Valeri CR, Borbone ML, Becker RC, et al. Increased Platelet Reactivity and Circulating Monocyte-Platelet Aggregates in Patients With Stable Coronary Artery Disease. *J Am Coll Cardiol.* 1998 Feb;31(2):352–8.
48. Ott I, Neumann FJ, Gawaz M, Schmitt M, Schoenig A. Increased Neutrophil-Platelet Adhesion in Patients With Unstable Angina. *Circulation.* 1996 Sept 15;94(6):1239–46.
49. Kindberg KM, Broch K, Andersen GØ, Anstensrud AK, Åkra S, Woxholt S, et al. Neutrophil Extracellular Traps in ST-Segment Elevation Myocardial Infarction. *JACC Adv.* 2024 Sept;3(9):101193.
50. Wong SL, Demers M, Martinod K, Gallant M, Wang Y, Goldfine AB, et al. Diabetes primes neutrophils to undergo NETosis, which impairs wound healing. *Nat Med.* 2015 July;21(7):815–9.
51. Sauter RJ, Sauter M, Reis ES, Emschermann FN, Nording H, Ebenhöch S, et al. Functional Relevance of the Anaphylatoxin Receptor C3aR for Platelet Function and Arterial Thrombus Formation Marks an Intersection Point Between Innate Immunity and Thrombosis. *Circulation.* 2018 Oct 16;138(16):1720–35.
52. Jayne DRW, Merkel PA, Schall TJ, Bekker P. Avacopan for the Treatment of ANCA-Associated Vasculitis. *N Engl J Med.* 2021 Feb 18;384(7):599–609.
53. Legendre CM, Licht C, Muus P, Greenbaum LA, Babu S, Bedrosian C, et al. Terminal Complement Inhibitor Eculizumab in Atypical Hemolytic–Uremic Syndrome. *N Engl J Med.* 2013 June 6;368(23):2169–81.

54. Hillmen P, Young NS, Schubert J, Brodsky RA, Socié G, Muus P, et al. The Complement Inhibitor Eculizumab in Paroxysmal Nocturnal Hemoglobinuria. *N Engl J Med*. 2006 Sept 21;355(12):1233–43.

Supplementary Information

The Supplementary Information contains detailed experimental methods, extended flow cytometric analyses, additional echocardiographic parameters, baseline phenotyping of mouse models, and supporting in vivo and in vitro data related to platelet–neutrophil interactions and NET formation.

Acknowledgements

We thank the imaging and animal core facilities at University Hospital Freiburg and University Medical Center Mannheim for excellent technical support. We also acknowledge the support of the Core Facility Live Cell Imaging Mannheim (LIMA; DFG INST 91027/10-1 FUGG) for confocal microscopy.

We are grateful to Denisa D. Wagner for critically reading the manuscript and for her valuable comments and constructive suggestions. We thank Heike Dietz, Rohit Chaudhari, and Xinyu Hu for their technical assistance and experimental support. We further thank all members of the participating laboratories for helpful discussions. Graphical illustrations were created using BioRender.com.

Funding

This work was supported by the Deutsche Forschungsgemeinschaft (DFG, German Research Foundation) in the SFB1366/2 (Project # 394046768) to H.F.L. and D.D. The Physician Scientist Program of the Helmholtz-Institute for Translational AngioCardioScience (HI-TAC) and the Carl Zeiss Foundation supported N.S. This work was furthermore supported by the Else-Kröner Fresenius Stiftung [Schlüsselprojekt, 2023_EKSE.46], the German Research Centre for Cardiovascular Research [partner site Mannheim/ Heidelberg, FKZ81Z0700110], the ERA PerMed 2020 JTC grant [“PROGRESS”]. L.A.H. is funded by the Berta-Ottenstein-Programme for Advanced Clinician Scientists, Faculty of Medicine, University of Freiburg.

Disclosure of interest

The authors declare no conflict of interest.

Author Contributions

H.F.L. and D.D. conceived the study and provided the overarching scientific framework. N.S. and S.Z. developed the experimental design. N.S. and S.Z. performed the experiments, analyzed and

interpreted the data, and contributed to manuscript preparation. N.S. coordinated the study, led the integration of experimental data, and drafted the initial version of the manuscript. H.N., J.v.E., P.S., and C.D.S. performed and supervised in vitro platelet–neutrophil co-culture experiments and contributed to data interpretation. H.N. and C.D.S. provided conceptual input and scientific oversight for the in vitro studies. M.S., Na.S., N.G., and M.A.H. contributed to experimental work, data acquisition, and technical support. N.B. contributed to baseline echocardiographic analyses, flow cytometry experiments, and data interpretation. K.K. contributed to study design and data interpretation. H.F.L. and D.D. jointly supervised the project, secured funding, and critically revised the manuscript. All authors discussed the results and approved the final version of the manuscript.

Figure Legends

Figure 1 | Platelet-specific *C5ar1* deletion improves post-infarction remodeling and cardiac function.

- (A) Experimental design of permanent left anterior descending (LAD) coronary artery ligation in $Pf4^{cre+} C5ar1^{fl/fl}$ mice and Cre-negative littermate controls, followed by serial echocardiography and terminal analyses up to day 14.
- (B) Representative transverse left ventricular sections stained with TTC on day 14 after myocardial infarction, with infarcted myocardium appearing white and viable myocardium appearing red. Infarcted areas are indicated by a solid white outline (scale bar = 2 mm).
- (C) Quantification of infarct size expressed as percentage of left ventricle (LV).
- (D) Representative M-mode echocardiographic images.
- (E) Echocardiographic assessment of left ventricular ejection fraction (EF; left) and fractional shortening (FS; right) on day 1 and day 13 after myocardial infarction.
- (F) Representative immunofluorescence images of collagen I (red) and DNA (DAPI, blue) on day 14.
- (G) Quantification of collagen I-positive area (collagen I, % of LV section).
- (H) Representative CD31 (green) immunostaining with DNA staining (DAPI, blue) in the peri-infarct region on day 14.
- (I) Quantification of capillary density (CD31-positive area, %).

Data are shown as mean \pm SD; each dot represents one mouse. $n = 4$ mice per group for TTC and immunofluorescence analyses; $n = 9-10$ mice per group for echocardiography. Statistical analysis was performed using one-way ANOVA for EF and FS and two-tailed unpaired t-tests for all other comparisons. $P < 0.05$, $P < 0.01$, $P < 0.001$.

Figure 2 | Platelet *C5ar1* deficiency increases circulating but limits myocardial platelet–neutrophil complexes and NET deposition.

- (A) Representative immunofluorescence images of peri-infarct myocardium stained for Ly6G (red) and CD42b (green) with DNA staining (DAPI, blue), showing myocardial platelet–neutrophil complexes (PNCs).
- (B) Quantification of myocardial PNC density (mm^{-2}) in the peri-infarct region (see also Supplementary Figure 10 for platelet and neutrophil infiltration).

- (C) Representative immunofluorescence images of peri-infarct myocardium stained for myeloperoxidase (MPO, red) and citrullinated histone H3 (H3Cit, green) with DNA (DAPI, blue), showing neutrophil extracellular traps (NETs).
- (D) Quantification of NET burden expressed as percentage of H3Cit⁺ area of the left ventricle (LV).
- (E) Flow cytometric gating strategy for platelet–neutrophil complexes (PNCs) in whole blood. Neutrophils were identified by Ly6G, and PNCs were defined as Ly6G⁺CD42b⁺ events.
- (F) Circulating PNCs expressed as percentage of CD42b⁺ events among Ly6G⁺ neutrophils on day 1 and day 14 after myocardial infarction in Pf4^{cre}+ C5ar1^{fl/fl} mice and Cre-negative littermate controls.
- (G) Spearman correlation analysis demonstrating an inverse relationship between circulating PNCs on day 1 after myocardial infarction and myocardial PNC density on day 14 across individual mice ($r = -0.83$, $P = 0.02$).

Data are shown as mean \pm SD; each dot represents one mouse. $n = 4$ mice per group for immunofluorescence analyses (A–D) and $n = 9$ mice per group for flow cytometric analyses (E–F). Statistical analysis was performed using two-tailed unpaired t-tests for immunofluorescence data, one-way ANOVA for flow cytometric analyses, and Spearman's rank correlation for association analysis (G). $P < 0.05$, $P < 0.01$, $P < 0.001$, $P < 0.0001$. Scale bars, 20 μm (A) and 10 μm (C).

Figure 3 | Platelet C5aR1 regulates α -granule biology and promotes CXCL4-dependent NET formation.

- (A) Representative single-plane confocal immunofluorescence images of fixed and permeabilized resting wild-type (WT) and C5aR1-deficient platelets stained for P-selectin (CD62P, green) and CXCL4 (red), illustrating altered α -granule organization.
- (B) Quantification of intracellular α -granule content per platelet, expressed as total area of P-selectin–positive granules and colocalized P-selectin/CXCL4 granules, measured by confocal microscopy. Data are shown as individual platelet values pooled from $n = 3$ independent experiments. Outliers were identified and removed using the ROUT method ($Q = 1\%$) prior to analysis.
- (C) Flow cytometric analysis of platelet surface P-selectin expression 24 h after myocardial infarction following ex vivo stimulation of whole blood with 100 nM phorbol 12-myristate 13-acetate (PMA), expressed as geometric mean fluorescence intensity (GMFI) of CD42b⁺ platelets.

- (D) Flow cytometric analysis of platelet integrin GPIIb/IIIa activation under the same conditions, expressed as percentage of activated GPIIb/IIIa among CD42b⁺ platelets.
- (E) Plasma CXCL4 concentrations after MI in Pf4^{cre+} C5aR1^{fl/fl} mice and Cre-negative littermate controls.
- (F) Schematic of the in vitro platelet–neutrophil co-incubation assay. WT or C5aR1-deficient platelets were stimulated with C5a and co-incubated with neutrophils, followed by confocal immunofluorescence staining for myeloperoxidase (MPO), citrullinated histone H3 (H3Cit), and DNA (DAPI) to assess NET formation, in the presence or absence of low-dose heparin or recombinant CXCL4 (rCXCL4).
- (G) Representative immunofluorescence images of neutrophils after co-incubation, stained for MPO (red), H3Cit (green), and DNA (DAPI, blue), illustrating NET formation under the indicated conditions (see Supplementary Figure 13 for neutrophil-intrinsic and platelet-mediated control conditions).
- (H) Quantification of NET formation expressed as percentage of H3Cit⁺ neutrophils.

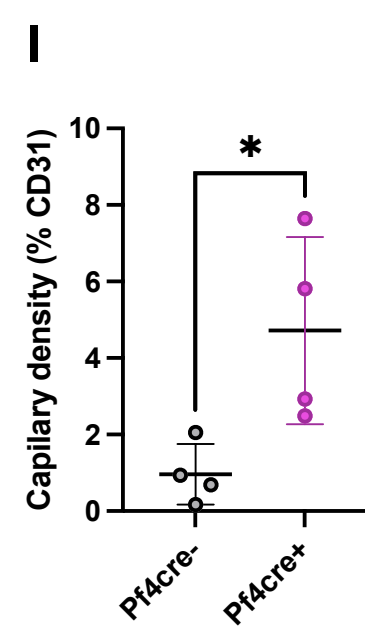
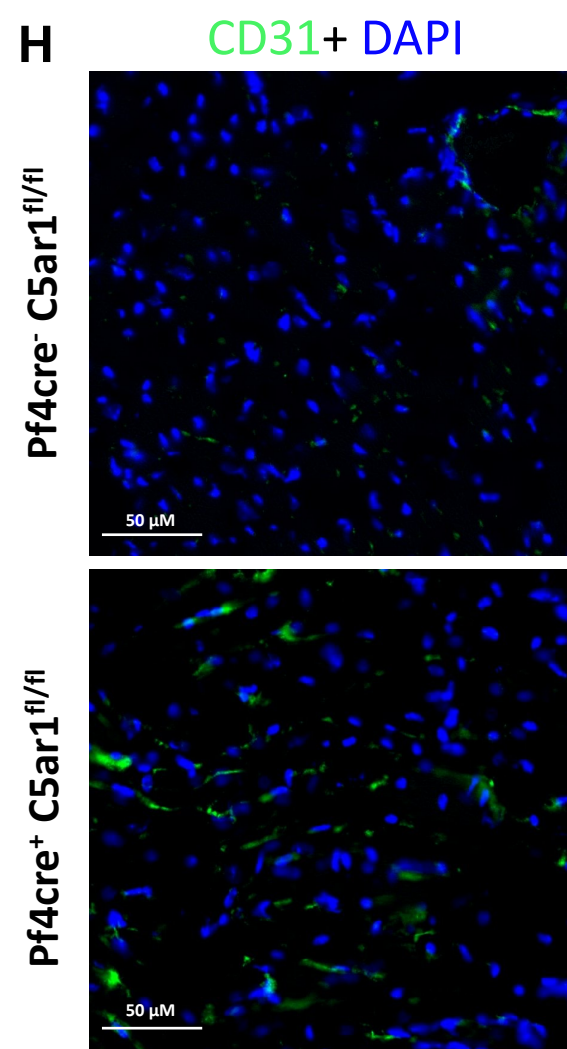
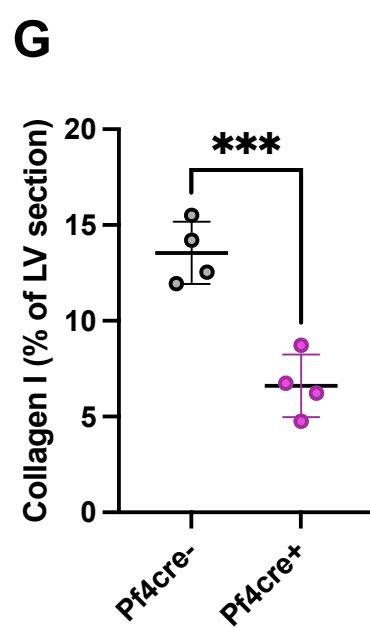
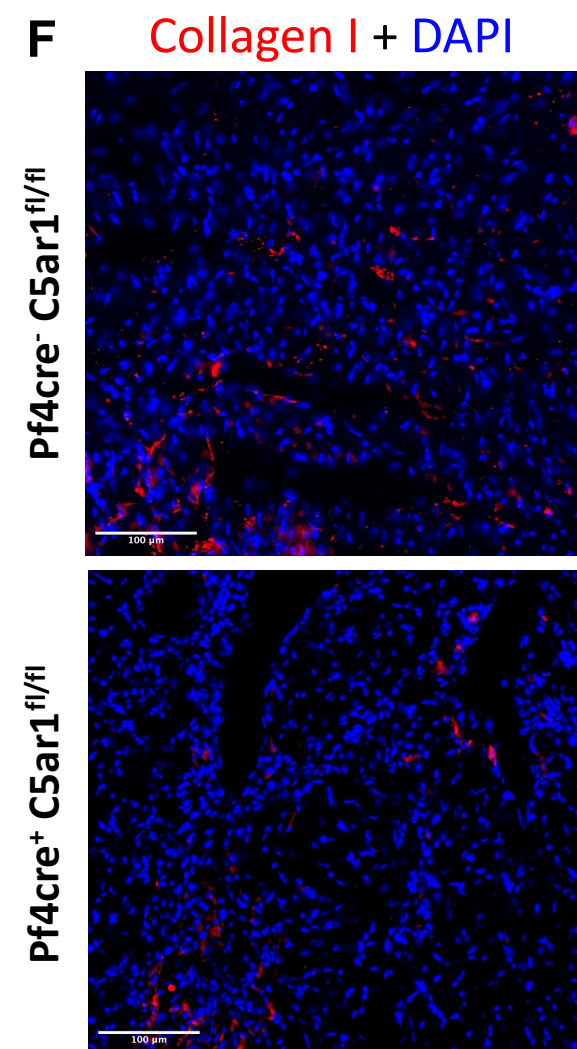
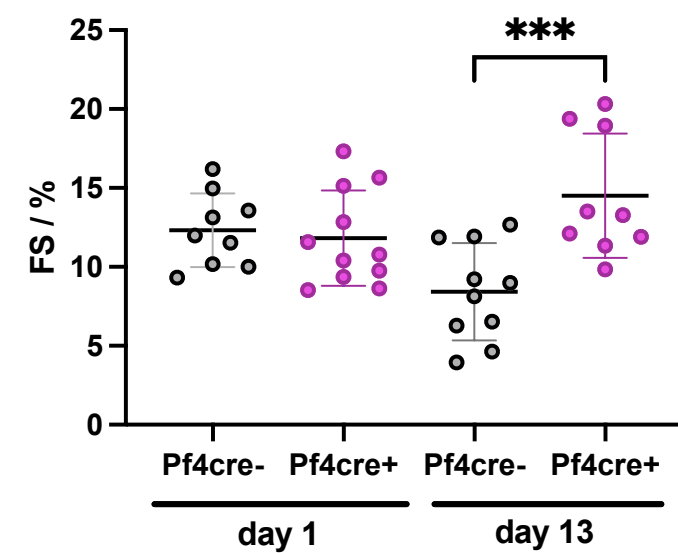
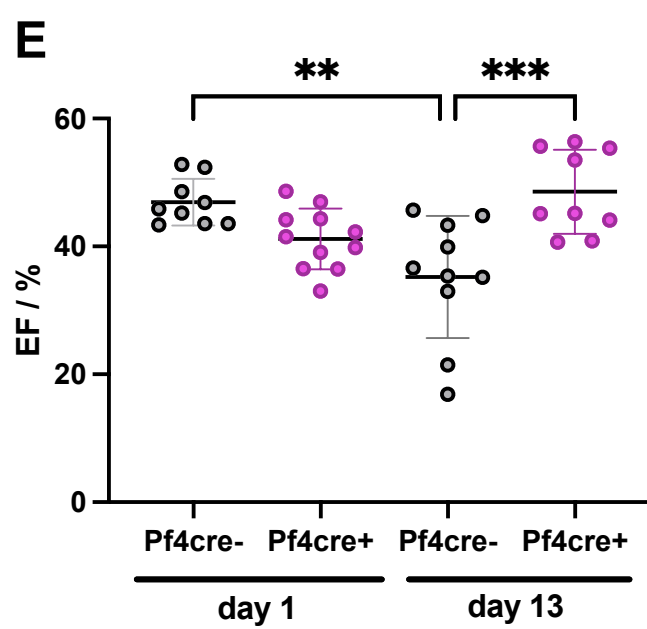
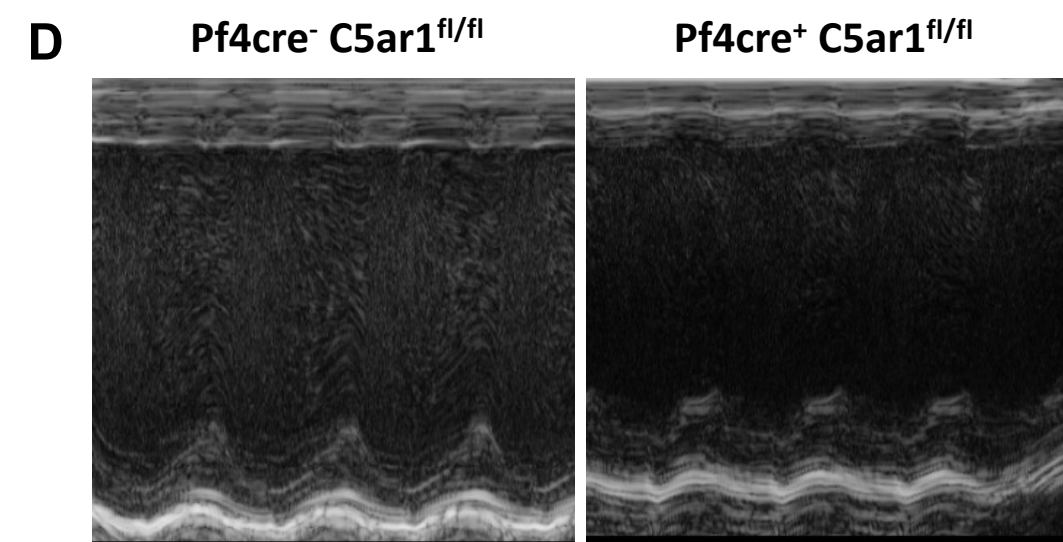
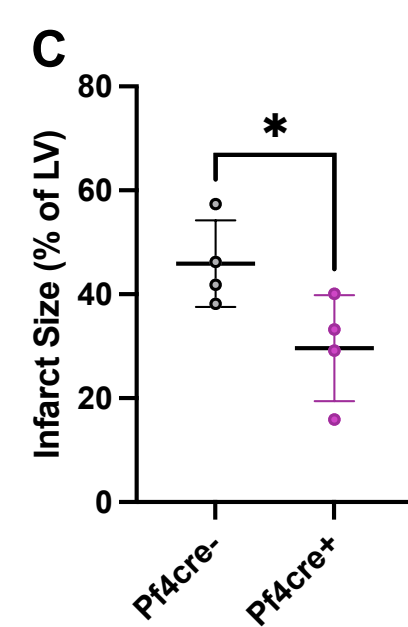
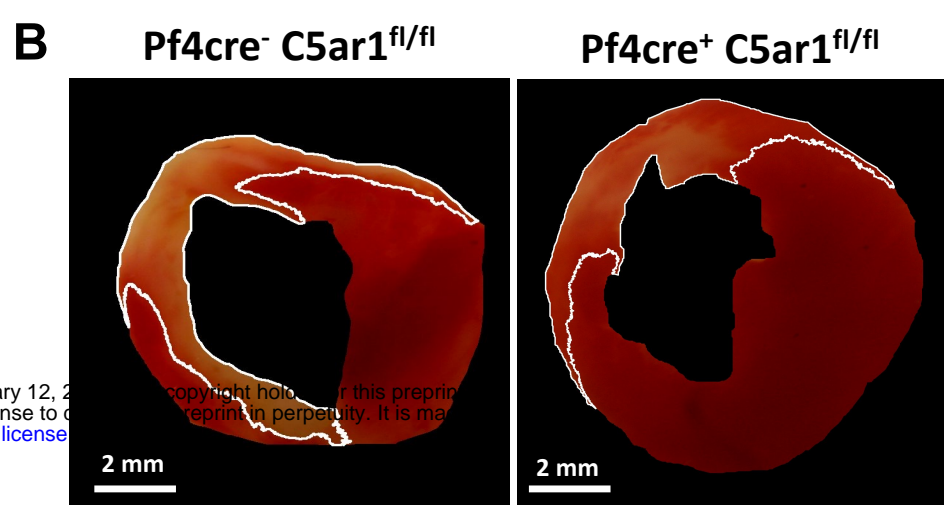
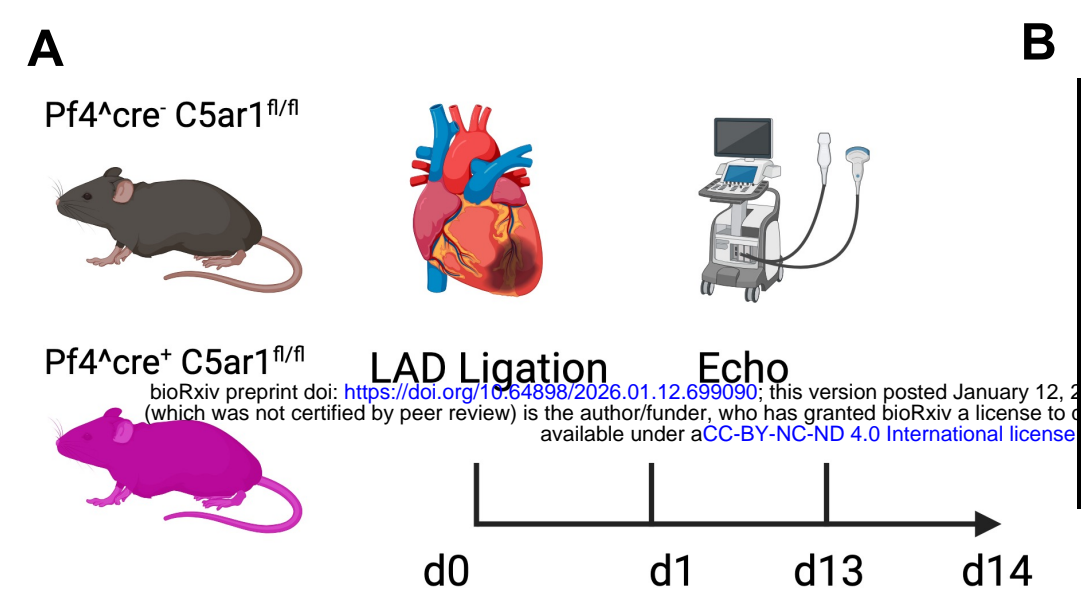
Data are shown as mean \pm SD unless otherwise indicated; each dot represents one biological replicate or mouse, as indicated. For α -granule analyses (A–B), data are shown as individual platelet values pooled from n = 3 independent experiments and analyzed using two-tailed unpaired t-tests following ROUT-based outlier exclusion (Q = 1%). Flow cytometry data (C–D) were analyzed using one-way ANOVA across time points and genotypes (see also Supplementary Figures for day 14 analyses). Plasma CXCL4 measurements (E) were analyzed using two-tailed unpaired t-tests. NET formation assays (H) were analyzed using one-way ANOVA with appropriate post hoc correction. P < 0.05, P < 0.01, P < 0.001, P < 0.0001. Scale bars, 2 μ m (A) and 20 μ m (G).

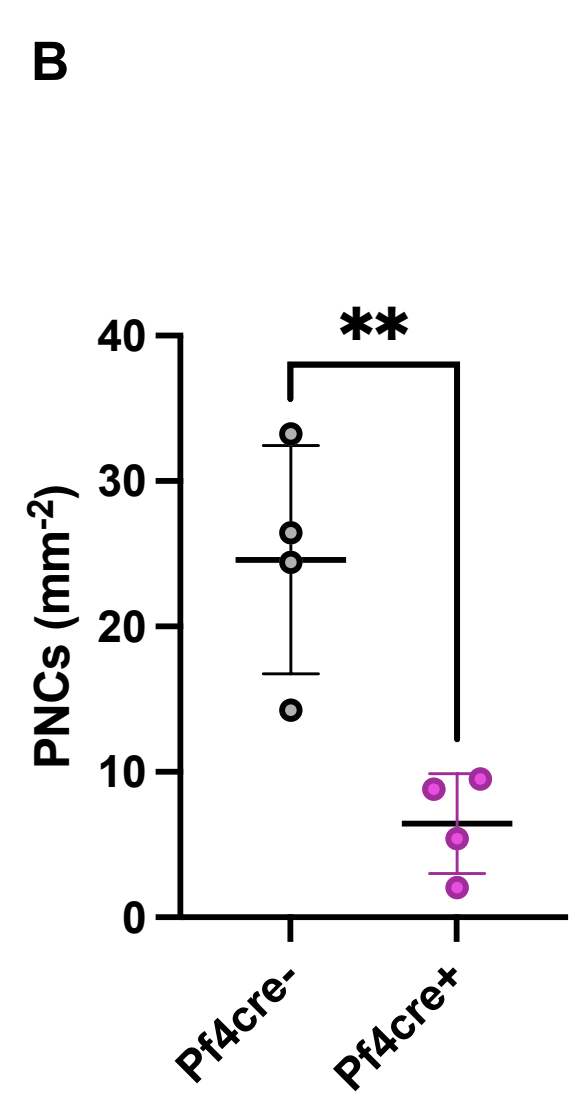
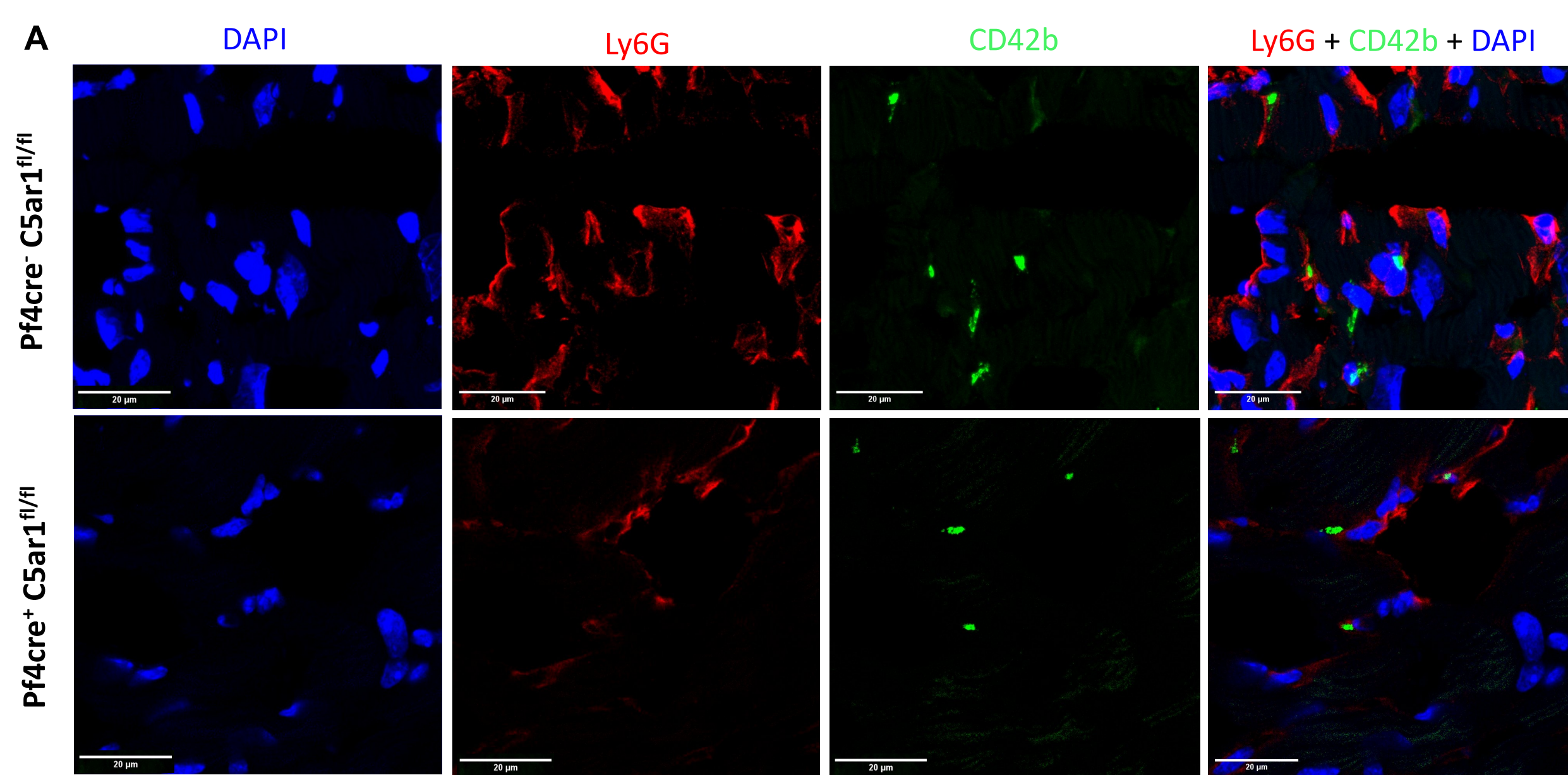
Figure 4 | C5aR1 inhibition with PMX205 phenocopies platelet-specific C5ar1 deletion.

- (A) Experimental design for daily subcutaneous administration of the C5aR1 inhibitor PMX205 or PBS for 14 days following permanent left anterior descending (LAD) coronary artery ligation.
- (B) Representative TTC-stained transverse left ventricular sections on day 14 after myocardial infarction, with infarcted myocardium appearing white and viable myocardium appearing red. Infarcted areas are indicated by a solid white outline (left). Corresponding quantification of infarct size, expressed as percentage of left ventricular (LV) area (right).

- (C) Quantification of collagen I-positive area in immunofluorescence staining, expressed as percentage of LV area.
- (D) Representative M-mode echocardiographic images on day 13 after myocardial infarction.
- (E) Echocardiographic assessment of left ventricular ejection fraction (EF; left) and fractional shortening (FS; right) on day 1 and day 13 after myocardial infarction.
- (F) Representative immunofluorescence images of peri-infarct myocardium stained for Ly6G (red) and CD42b (green) with DNA (DAPI, blue), illustrating myocardial platelet-neutrophil complexes (PNCs).
- (G) Quantification of myocardial PNC density (mm^{-2}).
- (H) Quantification of myocardial NET burden expressed as percentage of H3Cit⁺ neutrophils.
- (I) Representative immunofluorescence images of peri-infarct myocardium stained for myeloperoxidase (MPO), citrullinated histone H3 (H3Cit), and DNA (DAPI), illustrating NET deposition.
- (J) Representative flow cytometry plots of platelet surface P-selectin expression and activated GPIIb/IIIa ($\alpha\text{IIb}\beta 3$) in PMA-stimulated whole blood 24 h after myocardial infarction.
- (K) Quantification of platelet surface P-selectin expression in PMA-stimulated whole blood 24 h after myocardial infarction.
- (L) Quantification of platelet GPIIb/IIIa activation in PMA-stimulated whole blood 24 h after myocardial infarction.

Data are shown as mean \pm SD; each dot represents one mouse. Statistical analysis was performed using two-tailed unpaired t-tests for infarct size and collagen I quantification (B, C) and for myocardial PNC and NET quantification (G, H). Echocardiographic parameters (E) and flow cytometric platelet activation analyses (K, L) were analyzed using one-way ANOVA across time points and treatment groups (see also Supplementary Information for day 14 analyses). $P < 0.05$, $P < 0.01$, $P < 0.001$, $P < 0.0001$. Gating strategies are provided in the Supplementary Information. Scale bars, 2 mm (B) and 20 μm (F, I).





bioRxiv preprint doi: <https://doi.org/10.64898/2026.01.12.699090>; this version posted January 12, 2026. The copyright holder for this preprint (which was not certified by peer review) is the author/funder, who has granted bioRxiv a license to display the preprint in perpetuity. It is made available under aCC-BY-NC-ND 4.0 International license.

